Journal of the European Ceramic Society 22 (2002) 479–485

www.elsevier.com/locate/jeurceramsoc

Fabrication of cordierite–mullite ceramic composites with differently shaped mullite grains

Junichi Takahashi*, Maya Natsuisaka, Shiro Shimada

Division of Materials Science and Engineering, Graduate School of Engineering, Hokkaido University N-13 W-8 Kita-ku, Sapporo 060-8628, Japan

Received 11 January 2001; received in revised form 28 March 2001; accepted 28 April 2001

Abstract

Cordierite–mullite composites were fabricated from various starting powder mixtures to study the effect of different mixing combinations of the starting materials (commercial oxide sols and/or hydroxide powders) on the resultant mullite grains in the sintered composites. The morphology of the mullite grains was substantially changed depending on the Al-source materials used. Acicular grains were produced from the alumina sol-containing mixtures, whereas the growth of angular or granular mullite grains occurred for the mixtures containing $Al(OH)_3$ powder. When using alumina sol, its higher reactivity combined with better dispersability in precursor powders could cause the lowering in the mullitization temperature than for those containing $Al(OH)_3$ powder. In addition, it could produce very fine mullite seed particles in a calcined powder, leading to the growth of the acicular mullite grains in the sintered C/M composites. © 2002 Elsevier Science Ltd. All rights reserved.

Keywords: Composites; Cordierite; Grain growth; Microstructure; Mullite

1. Introduction

Cordierite ceramics have the excellent property of thermal shock resistance. It enables them to be used under a severe environment of very rapid heating and cooling conditions. Recently, ceramic filter elements have been increasingly required for removal of particulates in several high temperature systems.[1] Cordierite ceramics, of course, are one of the candidate materials for high temperature filtration applications.[1–3] However, the relatively poor mechanical properties that are inherent to cordierite ceramics should be improved to obtain long-term structural durability. A possible enhancement of its mechanical strength is to add a reinforcing phase and fabricate a ceramic composite.

Cordierite-mullite (C/M) composites have been produced from various starting materials.[4–12] Monroe et al.[8] and Anderson et al.[9] fabricated C/M composites from mixtures of commercially available cordierite, mullite and glass powders and studied some physical properties of the composite samples. Densification of C/M composites at much lower temperatures was achieved using precursor powders prepared via sol-gel routes.[7,11] However, little information on the morphology of the mullite grains grown during sintering was reported in these studies. Mussler et al. fabricated C/M composites with various mullite contents by mechanical mixing of preformed powders of cordierite glass and mullite and subsequent heating of the corresponding pellets at temperatures from 800 to 1650°C in different atmospheres.[4] They found that the directional growth of mullite grains occurred after sintering at 1550°C, resulting in the evolution of coarse-grained acicular microstructure. Alternatively, sintering of a calcined powder mixture of preheated Al_2O_3, $Mg(OH)_2$ and anhydrous SiO_2 at a lower temperature (1450°C) caused the formation of angular mullite grains with a small aspect ratio of 2–3.[5] The effect of the C:M ratio in the composites on the morphology of the resulting mullite grains was described in a study using composite sols, in which acicular grains in the mullite-rich composite changed to equiaxed grain morphology with an increasing cordierite content.[12] Thus the C/M composites can be expected to have characteristic microstructure containing elongated mullite grains with various aspect ratios as a reinforcing phase. The different morphologies of mullite grains formed during

---

* Corresponding author. Fax: +81-11-706-6572.
E-mail address: tkjun@eng.hokudai.ac.jp (J. Takahashi).

PII: S0955-2219(01)00312-0

the sintering process would be essentially dependent on the starting powder, sintering temperature and liquid phase formed during sintering. In this study, to investigate the effect of mixing combinations of the different starting materials on the morphological change of mullite grains, C/M composites have been fabricated from various starting powder mixtures and the resulting microstructure has been evaluated. Our final goal with the C/M composites is to establish a method for controlling the morphology and content of mullite grains, which leads to the fabrication of toughened C/M composites.

2. Experimental

The starting materials used in this study were commercially available chemicals; Alumina sol[1] or $Al(OH)_3$ powder[2], and Silica sol[3] or SiO_2 powder[4] were used as the Al- and Si-sources, respectively. $Mg(OH)_2$ powder[5] was simultaneously added for the production of the cordierite phase.

Table 1 shows starting mixtures examined in the present study (hereafter referred to as precursor powders) and their mixing combinations of each material. At first, required amounts of the corresponding materials were weighed to obtain the fixed C:M compositions and mixed under each condition. The M-sol precursor powder was prepared by stirring both sols and $Mg(OH)_2$ powder with an appropriate amount of distilled water for several hours and microwave-drying. For the other precursor powders, given amounts of the corresponding starting materials were wet-mixed in a plastic container using yttrium-stabilized ZrO_2 (YSZ) balls and oven-dried. These precursor powders were calcined at 1300°C for 4 h and then ball-milled to obtain fine powders for sintering. Green compacts formed by uniaxial and isostatic pressing were sintered in the temperature range 1435–1445°C for 10 h. X-ray powder diffractometry (XRD) was used to identify the solid phases formed after calcination and sintering. Microstructural observation with scanning electron microscope (SEM, Jeol JSM-6300F) was conducted for calcined powders or sintered and polished composite samples. Transmission electron microscope (TEM, Jeol 2000ES) with EDS (energy dispersive X-ray spectroscope) was also used for the estimation of solid phases formed in the composite samples. Samples for TEM analysis were prepared by mechanical grinding and subsequent ion thinning using Ar gas (Gatan, Model 691).

Table 1
Combinations of each source material for precursor powders

	M-sol	A-sol	S-sol	Non-sol
Al-source	Alumina sol	Alumina sol	$Al(OH)_3$	$Al(OH)_3$
Si-source	Silica sol	SiO_2 powder	Silica sol	SiO_2 powder
Mg-source	$Mg(OH)_2$	$Mg(OH)_2$	$Mg(OH)_2$	$Mg(OH)_2$

3. Results and discussion

3.1. Fabrication and microstructure of M35 composites

Fig. 1 shows typical XRD profiles of a composite powder with a starting composition of C:M = 0.65:0.35 (molar fraction, referred to as the M35 composite) which was prepared from the M-sol precursor and heated in the temperature range from 1000 to 1300°C in air. The formation of spinel (marked by ○) with low crystallinity, which might be $MgAl_2O_4$ and Al,Si-spinel,[13,14] are recognized in the sample calcined at 1000 °C. On heating at elevated temperatures, diffraction peaks of mullite (M) and cristobalite (□) can be seen for samples calcined at 1200°C. The cordierite phase was formed after heating at 1300°C, where four crystalline phases co-existed with a decreasing relative content of cordierite > mullite ≈ cristobalite > spinel. The formation of the cordierite phases (μ- and α-) has been studied using a precursor powder derived via sol-gel route, in which the hydrolysis and subsequent dehydration and

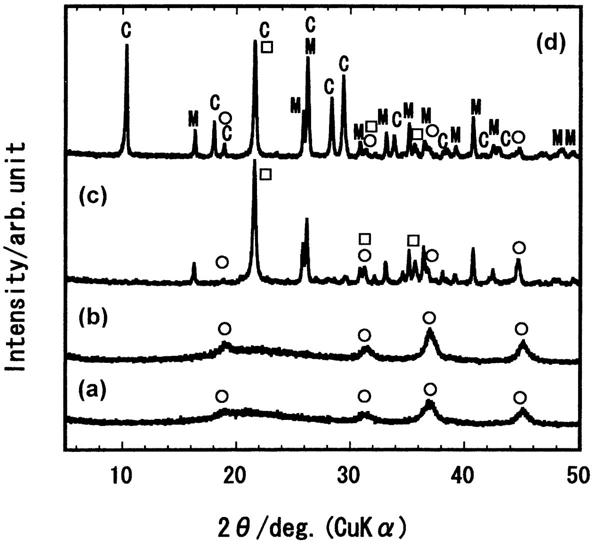

Fig. 1. X-ray diffraction profiles of M-sol powders calcined at (a) 1000°C, (b) 1100 °C, (c) 1200°C and (d) 1300°C. (C: cordierite, M: mullite, ○: spinel, □: cristobalite).

---

[1] Produced by Nissan Chemical Industries; $\eta \fallingdotseq 10^3$·mPa s at 20°C, fibrous particles with $d_{ave} \fallingdotseq 10 \times 100$ nm, amorphous by XRD.

[2] By High Purity Chemicals Lab.; 99.9% (purity).

[3] By Nissan Chemical Industries; $\eta \fallingdotseq 2$ mPa s at 20°C, colloidal particles with $d_{ave} = 10–20$ nm.

[4] By Kanto Chemical Co.; precipitated powder, amorphous by XRD.

[5] By High Purity Chemicals Lab.; 99.9% (purity).

condensation processes of metal alkoxides were controlled.[15,16] It was found that well crystallized α-cordierite was obtained after heat-treatment at 1200–1300°C, mainly depending on the hydrolysis conditions of starting metal alkoxides.[15] In the present composite powder, the α-cordierite phase could be formed at 1300°C from a mechanical mixture of alumina and silica sols and $Mg(OH)_2$ powder. This result suggested that the co-existing mullite phase had no significant effect on the formation temperature of α-cordierite in the M-sol powder. Relative phase changes with calcining temperature are given in Fig. 2 for all the precursor powders prepared. The formation behavior of each phase was somewhat dependent on the precursor powders. It should be noticed that mullite was formed at 1200°C for the M-sol and A-sol samples and the contents of the mullite phase in those samples heated at 1300°C was greater than those in the S-sol and non-sol samples.

Mullitization temperature in samples obtained from various starting materials widely differed due to the effect of impurities, firing atmosphere and the presence of pre-treatment. Okada et al. summarized the mullitization from various starting materials and showed that the formation temperature changed depending mainly on their particle sizes in the case of mixtures of sols or oxide powders.[17] In this study, the different mullitization behavior that could distinguish the M-sol and A-sol precursor group from the S-sol and non-sol group was due to the difference in the Al-source materials used. That is, the mullitization temperature was lowered by 100°C for the precursor powders containing alumina sol. This result implied that the size of alumina particles prepared by the thermal decomposition of the $Al(OH)_3$ powder in the S-sol and non-sol precursors might be larger than that derived from alumina sol. Probably this could be caused by insufficient or inhomogeneous mixing of the $Al(OH)_3$ powder in the starting non-sol and S-sol mixtures.

Typical microstructures of the M35 composites sintered at 1440 °C for 10 h are shown in Fig. 3. Mullite grains grown during sintering can be seen as brightened grains dispersing in a cordierite matrix. As shown in Fig. 3, the morphology of the mullite grains could be conventionally classified into two types. Acicular grains grew in both the M-sol and A-sol samples. On the other hand, angular or granular mullite grains were distributed in the composites derived from the non-sol and S-sol powders. The comparative examination of those mullite grains was made between the M-sol and non-sol derived composites. Fig. 4 shows the distributions of (A) grain size (based on the smaller dimension of an elongated grain) and (B) aspect ratio of the mullite grains for the samples sintered at 1435 and 1445°C. The average size of the mullite grains in the M-sol samples was much smaller than that in the non-sol sample. Surprisingly, a slight increase in sintering temperature by 10°C caused the considerably increasing size of mullite grain in both samples, suggesting the accelerated grain growth by liquid phase. Lattice parameters of mullite formed at 1445°C were calculated to estimate the composition of the mullite grains in both samples. They were (1) $a_0 = 0.7535$ nm, $b_0 = 0.7703$ nm, $c_0 = 0.2885$ nm and (2) $a_0 = 0.7550$ nm, $b_0 = 0.7697$ nm, $c_0 = 0.2886$ nm for the M-sol and non-sol samples, respectively. According to

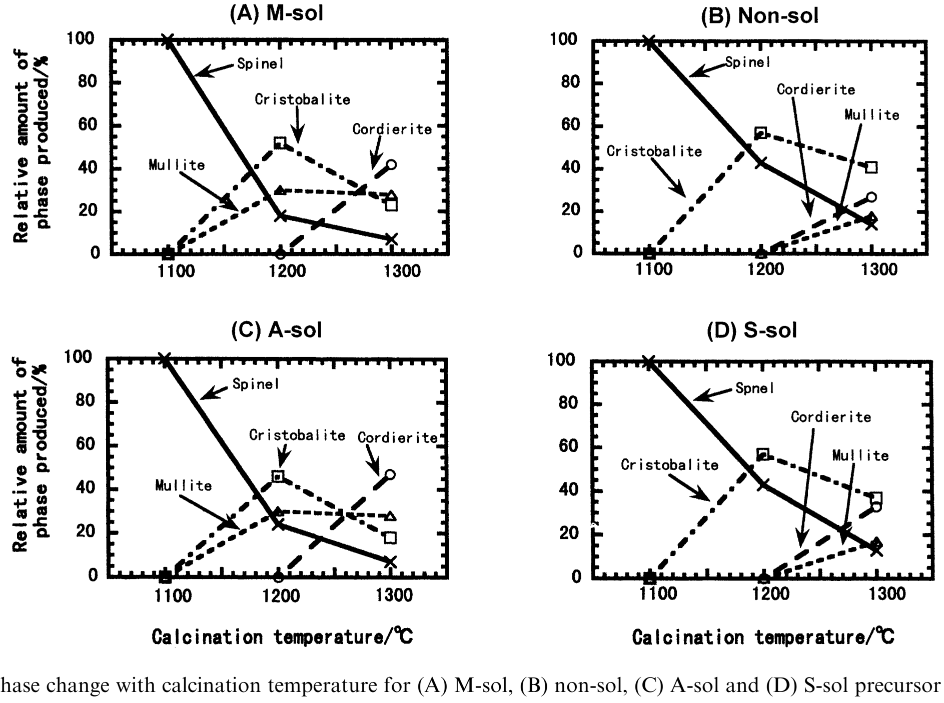

Fig. 2. Phase change with calcination temperature for (A) M-sol, (B) non-sol, (C) A-sol and (D) S-sol precursor powders.

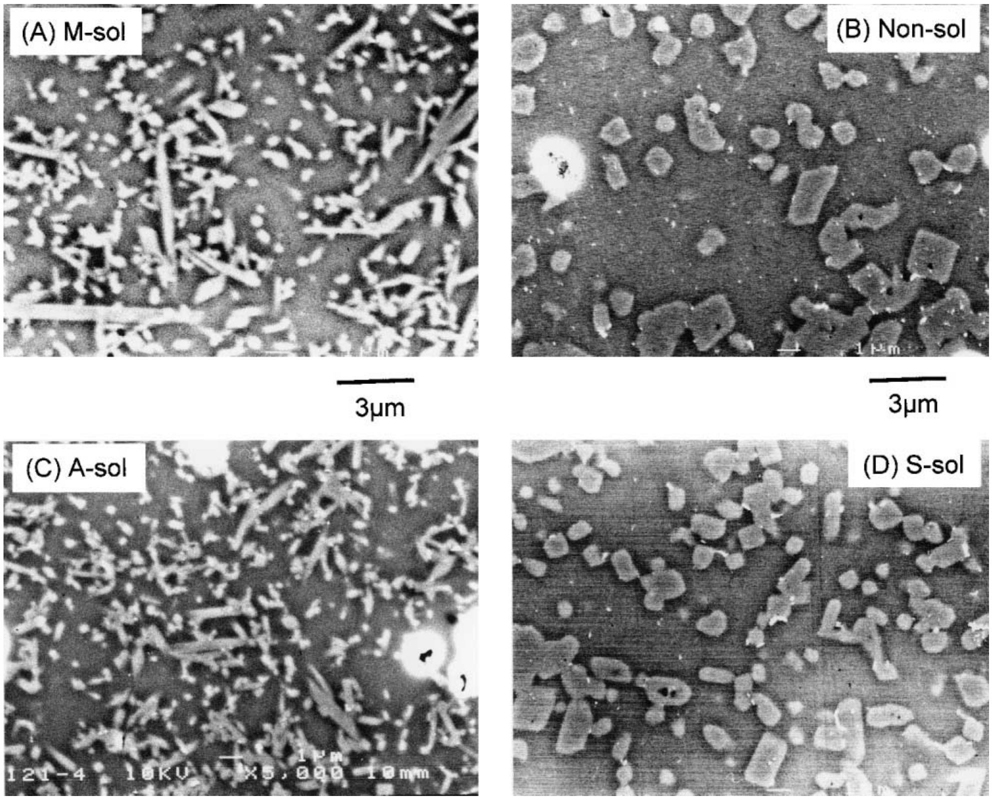

Fig. 3. SEM images of polished surfaces of M35 composites derived from (A) M-sol, (B) non-sol, (C) A-sol and (D) S-sol powders.

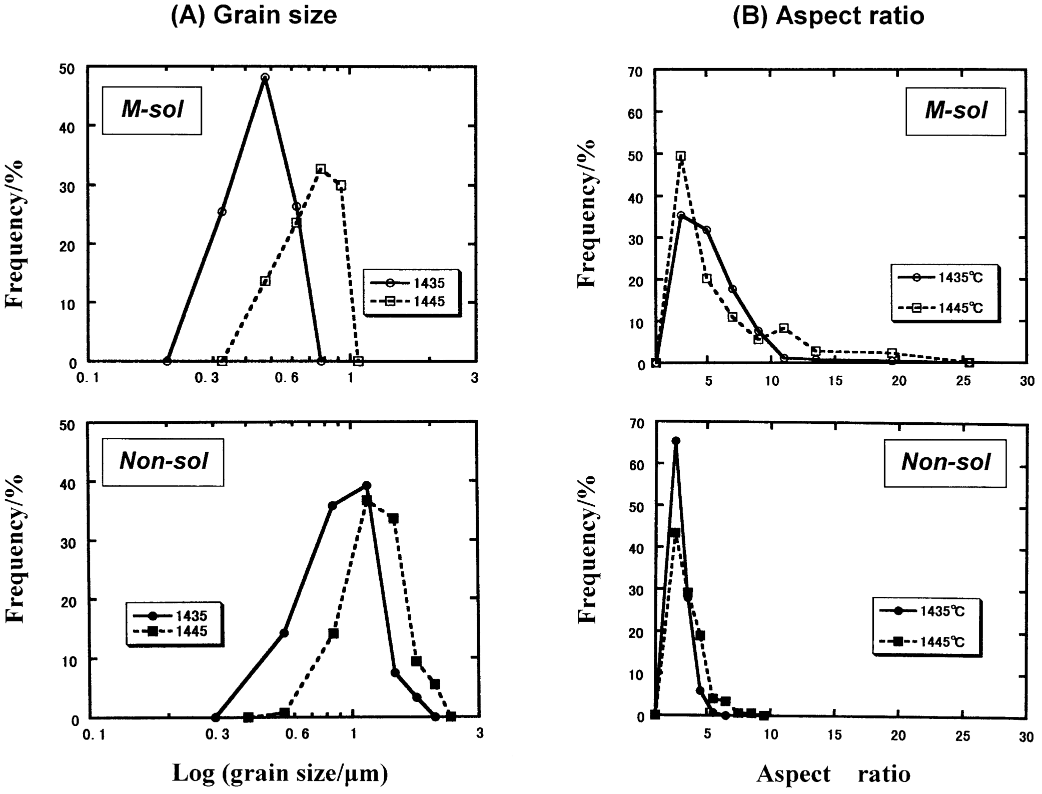

Fig. 4. Distributions of (A) size and (B) aspect ratio of mullite grains grown in the sintered M-sol and non-sol composites.

the relationship between the a_0 lattice parameter and composition of mullite,[18,19] the compositions of mullite in the M-sol and Non-sol samples might be evaluated to be approximately 71.5 wt% and 73.0 wt.% Al_2O_3, respectively.

In addition to the grains size, the distribution curves of the aspect ratio of mullite grains substantially differed between both samples. The curves of the M-sol composite expand and tail up to the ratio of 20, whereas the non-sol samples show very narrow curves with a maximum ratio of 2. An increase in sintering temperature, however, had little effect on the distribution curve of the aspect ratio for both samples. As can be deduced from Fig. 3, the distribution characteristics of the size and aspect ratio of the mullite grains in the A-sol and S-sol composites were similar to those in the M-sol and non-sol composites, respectively. The morphology and size of the resulting mullite grains were hardly affected by calcination temperature prior to sintering for all the composites derived from different precursor powders.

3.2. *Effect of starting materials on the morphology of mullite grains*

Appreciable difference in the formation behavior of crystalline phases after calcination was the temperature at which mullitization occurred (Fig. 2). Obviously, the mullitization temperature was lowered in the precursor powders containing alumina sol, i.e. the M-sol and A-sol samples. Several mullitization routes are known and the mixing states of SiO_2 and Al_2O_3 components in the starting materials determine the reaction process.[17] In the present study, mullite was formed via a similar reaction sequence irrespective of the different mixing combinations of the starting materials, because no additional phase was detected in the calcined samples. The sequence was considered to be amorphous → Al,Si-spinel → mullite. Probably, higher reactivity and better dispersability of alumina sol in the M-sol and A-sol precursor powders might cause the formation of mullite at a lower temperature. Fig. 5 shows SEM images of calcined (1300 °C) and ground particles of the M-sol and Non-sol samples. The image of the M-sol sample [Fig. 5(A)] reveals a dense and single particle in appearance, which was the morphological feature of particles prepared via the sol-gel route. In addition, it should be noticed that the single particle definitely consisted of different solid phases as indicated in Fig. 2. These results suggested that fibrous particles of alumina sol of 10×100 nm in size reacted with colloidal particles of silica sol having an average diameter of 10–20 nm (morphologies and sizes of alumina and silica sols were based on TEM observation) to form very fine mullite seed crystals that should distribute in a single M-sol particle as shown in Fig. 5(A). Consequently, this would lead to the formation of the acicular mullite grains after sintering. On the contrary, the Non-sol sample was characterized by the coagulation of small primary particles, each of which corresponded to different solid phases formed by calcination [Fig. 5(B)]. Obviously, the sizes of those primary particles were larger than those contained in the calcined M-sol particle in Fig. 5(A). Sintering of a green compact consisting of these coagulated non-sol particles caused the growth of the angular or granular mullite grains in the composites. Thus, difference in the reactivity and dispersability between alumina sol and $Al(OH)_3$ powder in the precursor mixtures definitely resulted in the different morphologies and sizes of the mullite grains grown during sintering.

In order to examine the effect of mixing procedure of the starting materials on the morphology of the resultant mullite grains, a C/M composite was fabricated by an alternative method using alumina and silica sols. Prior to the mixing process, cordierite and mullite precursor powders were separately prepared using each sol and calcined at 1300°C to form the corresponding oxide powders. Then, each of the preformed and ground oxide powders were mechanically mixed, pressed into a disk and sintered at 1440°C. The microstructure of the sintered composite with C:M = 0.5:0.5 can be seen in Fig. 6. The morphology of the mullite grains observed in Fig. 6 is basically angular and found to be similar to that observed not in

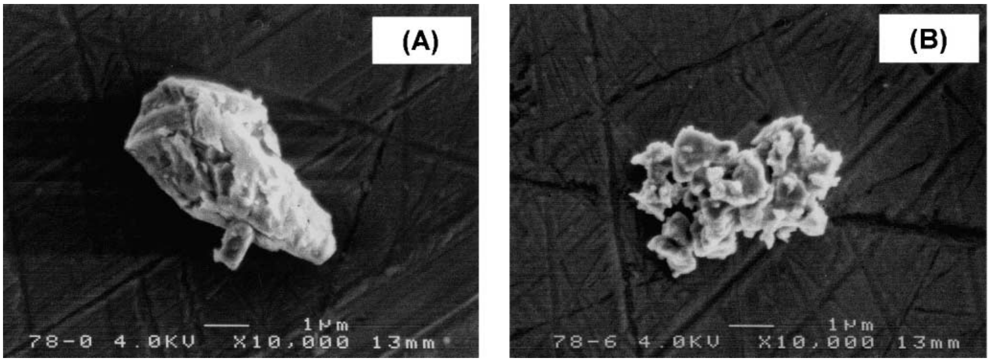

Fig. 5. Morphology of a calcined and ground particle of (A) M-sol and (B) non-sol precursor powders.

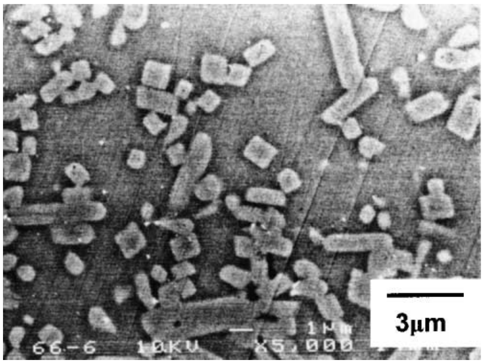

Fig. 6. Microstructure of M50 composite with angular mullite grains.

the M-sol (A-sol) but in the non-sol (S-sol) composite. This result supported the facet that the size and dispersed state of the mullite particles preformed during calcination at 1300°C was substantially different between the M-sol and non-sol powders; very fine mullite microcrystals were dispersed in a dense and single M-sol particle together with the other solid phases [Fig. 5(A)], whereas relatively larger mullite particles constituted an aggregated Non-sol particle [Fig. 5(B)]. Therefore, it might be concluded that the size and dispersed state of the mullite particles in a green compact was responsible for the resulting morphology of the mullite grains in the sintered composite.

Although it could be explained that elongation of the mullite grains in the sintered composite is attributed to the presence of a liquid phase during sintering, there have been few examinations on the morphological change of the mullite grains in relation to the amount and/or composition of the liquid phase formed. To assure the formation of a liquid phase in the present study, a C/M composite with a SiO_2-rich composition (theoretically C:M = 0.5:0.5 with 12 mol% excess SiO_2) was sintered (1440°C) from the M-sol precursor. ATEM microphotograph of the thinning-treated sample is given in Fig. 7. It reveals elongated mullite grains ("M" in Fig. 7) and a glassy phase ("G") composed of more than 95% SiO_2. According to the phase diagram of the system $MgO–Al_2O_3–SiO_2$, the lowest temperature at which a liquid phase is formed near the cordierite composition is 1345°C.[20] In each powder calcined at 1300°C, there existed the cristobalite and spinel particles in addition to the cordierite and mullite particles. Therefore, local inhomogeneity in the mixing state of each constituting solid particle might occur in a green body, causing the formation of liquid phase during sintering process. The amount and composition of a liquid phase formed must be dependent on the overall composition of the composite and sintering temperature. A relationship between a liquid phase and the resultant morphology of the mullite grains will be examined in a successive study.

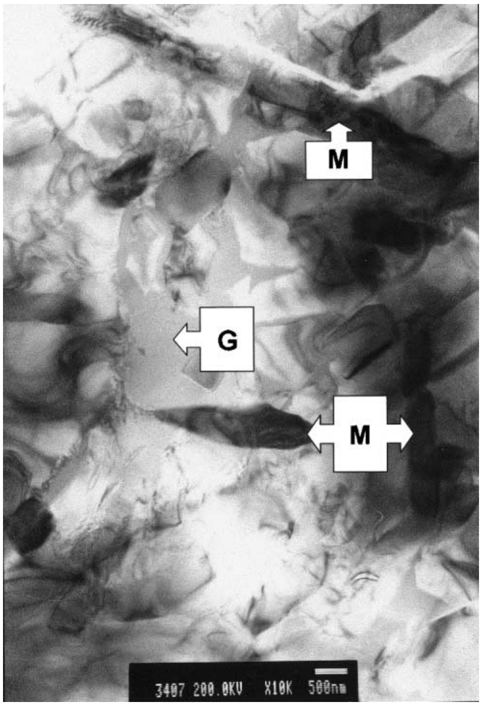

Fig. 7. TEM micrograph of SiO_2-rich M50 composite showing elongated mullite grains (M) and a glassy phase (G).

4. Conclusion

Cordierite–mullite composites (a composition of C:M = 0.65:0.35 in molar fraction) were fabricated from various precursor powders prepared using different starting materials (alumina sol and $Al(OH)_3$ powder, silica sol and SiO_2 powder and $Mg(OH)_2$ powder as the Al-, Si- and Mg-source materials, respectively). Required amounts of the corresponding materials were weighed and mixed under appropriate conditions to obtain a precursor powder having the fixed final composition. From solid phase identification on the calcination of each precursor powder, mullitization temperature was lowered for precursor powders containing alumina sol (the M- and A-sols). Microstructural observation of the sintered compacts revealed that acicular mullite grains with a maximum aspect ratio of 20 grew in the M-sol and A-sol derived composites, whereas angular or granular mullite grains having very small aspect ratios were distributed in the composites obtained from the non-sol and S-sol powders. The higher reactivity and better dispersability of alumina sol in precursor powders could cause the lowering in mullitization temperature and the production of very fine mullite seed particle in a calcined powder, leading to the growth of the acicular mullite grains in the sintered C/M composites. Thus the size and dispersing state of the mullite particles in a green compact was responsible for the resulting morphology of the mullite grains in the sintered composite.

Acknowledgements

This study was partly supported by Japan Society for the Promotion of Science, Grant-in-Aid for Scientific Research (B), No.12450348, 2000.

References

1. Alvin, M. A., Lippert, T. E. and Lane, J. E., Assessment of porous ceramics materials for hot gas filtration applications. *Am. Ceram. Soc. Bull.*, 1991, **70**, 1491–1498.
2. Higashi, K. and Maeno, H., The latest status of the development of the advanced ceramic tube filter. *Reports Res. Lab. Asahi Glass Co., Ltd.*, 1992, **42**, 81–95.
3. Takahashi, J., Kawai, Y. and Shimada, S., Hot corrosion of cordierite ceramics by Na- and K-salts. *J. Eur. Ceram. Soc.*, 1998, **18**, 1121–1129.
4. Mussler, B. H. and Shafer, M. W., Preparation and properties of mullite-cordierite composites. *Am. Ceram. Soc. Bull.*, 1984, **63**, 705–714.
5. Ikawa, H., Watanabe, T., Urabe, K. and Udagawa, S., Thermal expansion and microstructure of cordierite and mullite composite. *J. Ceram. Soc. Jpn.*, 1985, **93**, 762–767 (in Japanese).
6. Rasch, H., Considering some thermal applications for cordierite and cordierite-mullite materials. *Ceram. Forum Int./Ber.DKG*, 1987, **64**, 454–458.
7. Suzuki, H. and Saito, H., Preparation of precursor powders of cordierite-mullite composites from metal alkoxides and its sintering. *J. Ceram. Soc. Jpn*, 1988, **96**, 659–665 (in Japanese).
8. Monroe, D. L., Wachtman Jr, J. B. and Gault, C., The mechanical properties of cordierite-mullite composites as a function of temperature. In *Euro-Ceramics, 3: Engineering ceramics Proceedings of the First European Ceramic Society Conference*, ed. G. de With et al. Elsevier Science, London, 1989, pp. 3.394–3.408.
9. Anderson, R. M., Gerhardt, R., Wachtman, J. B. Jr., Onn, D. and Beecher, S., Thermal, mechanical, and dielectric properties of mullite-cordierite composites. In *Advances in Ceramics, 26; Ceramic substrates and Packages for Electronic Applications Proceedings of the International Symposium on Ceramic Substrates and Packages*, ed. M. F. Yan et al. The Am. Ceram. Soc, Westerville, 1989, pp. 265–277.
10. Hodge, J. D., Microstructure development in mullite-cordierite ceramics. *J. Am. Ceram. Soc.*, 1989, **72**, 1295–1298.
11. Srikanth, V., Ravindranathan, P., Rani, L. and Roy, R., Mullite-cordierite composites by triphasic sol-gel route. In *Metal and Ceramic Matrix Composites: Processing, Modeling and Mechanical Behavior*, ed. R.B. Bhagat, et al. The Minerals, Metals and Materials Soc., 1990, pp. 167–176.
12. Ismail, M. G. M. U., Tsunatori, H. and Nakai, Z., Preparation of mullite cordierite composite powders by the sol-gel method: its characteristics and sinterin. *J. Am. Ceram. Soc.*, 1990, **73**, 537–543.
13. Suzuki, H. and Saito, H., Processing of ultrafine mullite powders through alkoxide route. *Ceram. Trans.*, 1990, **6**, 263–274.
14. Mitachi, S., Matsuzawa, M. and Kaneko, K., Characterization of SiO_2–Al_2O_3 powders prepared from metal alkoxides. *Ceram. Trans.*, 1990, **6**, 275–286.
15. Suzuki, H., Ota, K. and Saito, H., Preparation of cordierite ceramics from metal alkoxides (part I). Preparation and characterization of the powder. *J. Ceram. Soc. Jpn.*, 1987, **95**, 163–169.
16. Pal, D., Chakraborty, A. K., Sen, S. and Sen, S. K., The synthesis, characterization and sintering of sol-gel derived cordierite ceramics for electronic applications. *J. Mater. Sci.*, 1996, **31**, 3995–4005.
17. Okada, K. and Otsuka, N., Formation process of mullite. *Ceram. Trans.*, 1990, **6**, 375–387.
18. Cameron, W. E., Composition and cell dimensions of mullite. *Am. Ceram. Soc. Bull.*, 1977, **56**, 1003–1011.
19. Klug, F. J., Prochazka, S. and Doremus, R. H., Alumina-silica phase diagram in the mullite region. *Ceram. Trans.*, 1990, **6**, 15–43.
20. Levin, E. M., Robbins, C. R. and McMurdie, H. F., *Phase Diagrams for Ceramists, vol. 1.* The Am. Ceram. Soc., Colombus, 1964, p. 712.